Photo- and Thermally Stimulated Luminescence Spectra of CdS$_{1-x}$Se$_x$ Nanocrystals Embedded in Borosilicate Glass

Yu.M. Azhniuk[1], V.V. Lopushansky[1], M.V. Prymak[1], K.P. Popovych[1], A.M. Solomon[1],
A.V. Gomonnai[1], D.R.T. Zahn[2]

[1] *Institute of Electron Physics, Ukrainian National Academy of Sciences,*
21, Universytetska st., 88017 Uzhhorod, Ukraine
[2] *Semiconductor Physics, Technische Universität Chemnitz, D-09107 Chemnitz, Germany*

Photoluminescence (PL) and thermally stimulated luminescence (TSL) of CdS$_{1-x}$Se$_x$ nanocrystals embedded in borosilicate glass are studied. The dependence of the spectral positions of the near-edge and surface-mediated PL bands on the nanocrystal composition and size is discussed. A different temperature behaviour for the higher-energy TSL band (maximum at 360-380 K, dependent of the nanocrystal size and composition) and the lower-energy peak (broad maximum in the range 350-450 K) is discussed.

Keywords: Semiconductor nanocrystals, Optical absorption, Photoluminescence, Thermally stimulated luminescence.

1. INTRODUCTION

Size-tunable photoluminescence (PL) of II-VI semiconductor nanocrystals is one of their most prominent optical properties resulting in their broad application range in nonlinear optics, optoelectronics, and biology [1-4]. In ternary nanocrystals (*e.g.* CdS$_{1-x}$Se$_x$), the luminescence features can be tuned in a wide spectral range by variation of both size and composition. A well known technique for obtaining CdS$_{1-x}$Se$_x$ nanocrystals is diffusion-limited growth in a glass matrix from a supersaturated solution [5, 6]. Extensive studies of stationary [5-16] and transient [17-19] PL properties of glass-embedded II-VI semiconductor nanocrystals were performed.

Thermally stimulated luminescence (TSL) studies provide additional information regarding radiative recombination centres in the semiconductor nanocrystals and at their interface with the host matrix. To our knowledge, only few experimental studies of TSL of glass-embedded II-VI nanocrystals were reported so far [20-22].

In this paper, we report on compositional and size variation of PL and TSL features in CdS$_{1-x}$Se$_x$ nanocrystals embedded in a borosilicate glass.

2. EXPERIMENTAL

The samples for the studies were prepared from a set of CdS$_{1-x}$Se$_x$ semiconductor-doped borosilicate glasses commercially available as optical cutoff filters for the yellow, orange, and red spectral range. Part of the samples were prepared directly from the filters. In order to prepare another part of the samples, a LZOS OS-14N filter was annealed at 1000 °C for 2 h. This resulted in the sample softening and complete dissolving of nanoparticles in the borosilicate glass (decolouring). After rapid quenching, each sample was cut into pieces which were subsequently subjected to thermal treatment at temperatures ranging from 625 to 675 °C, duration being varied from 2 to 12 h. This should result

in the precipitation of semiconductor nanocrystals from the supersaturated solution. The thermal treatment temperature was kept constant with an accuracy of ± 5 °C at the initial thermal stabilization stage and within ± 0.5 °C after the stabilization having been achieved. Formation of the nanocrystals was visually evidenced by the samples colouring, the colour and intensity depending on the thermal treatment temperature and duration. The details of the diffusion-limited growth technique are given in Refs. 23 and 24.

Optical absorption spectra were measured using a LOMO MDR-23 monochromator and a FEU-100 phototube with a resolution better than 2 nm.

PL measurements were carried out using a Dilor XY 800 spectrometer with a CCD camera and a He-Cd laser ($\lambda_{exc} = 441.6$ nm) for excitation. Optical measurements were performed at room temperature.

Spectrally resolved TSL measurements were performed for X-ray irradiated (800-1000 Gy) samples using a setup with a heating unit and control module similar to that of Ref. 25. The spectral TSL dependence was recorded using a MS7504i spectrograph with a Hamamatsu HS101H CCD camera. The TSL spectra were measured in the range of 650-850 nm. The samples under study were heated at a rate 0.4 K/s. The TSL spectra were recorded not later than 1 h after the X-ray irradiation.

3. RESULTS AND DISCUSSION

The chemical composition of the CdS$_{1-x}$Se$_x$ nanocrystals was determined from Raman scattering spectra [13, 24]. Optical absorption spectra of the samples, shown by short-dashed lines in Fig. 1, enabled us to determine the average nanocrystal size using the effective mass approximation [23].

As seen from Fig. 1, in the PL spectra of the glass-embedded CdS$_{0.2}$Se$_{0.8}$ nanocrystals two maxima are revealed, shifting towards lower energies with increasing nanocrystal size. A relatively narrow (0.1-0.2 eV) higher-energy PL maximum is located slightly below

the first absorption peak energy corresponding to the transition between $1s_e$ electron and $1S_{3/2}$ hole states (HOMO-LUMO transition) [26, 27] in the nanocrystals. The near-bandgap emission peak is often explained in a "dark exciton" model taking into account the exciton
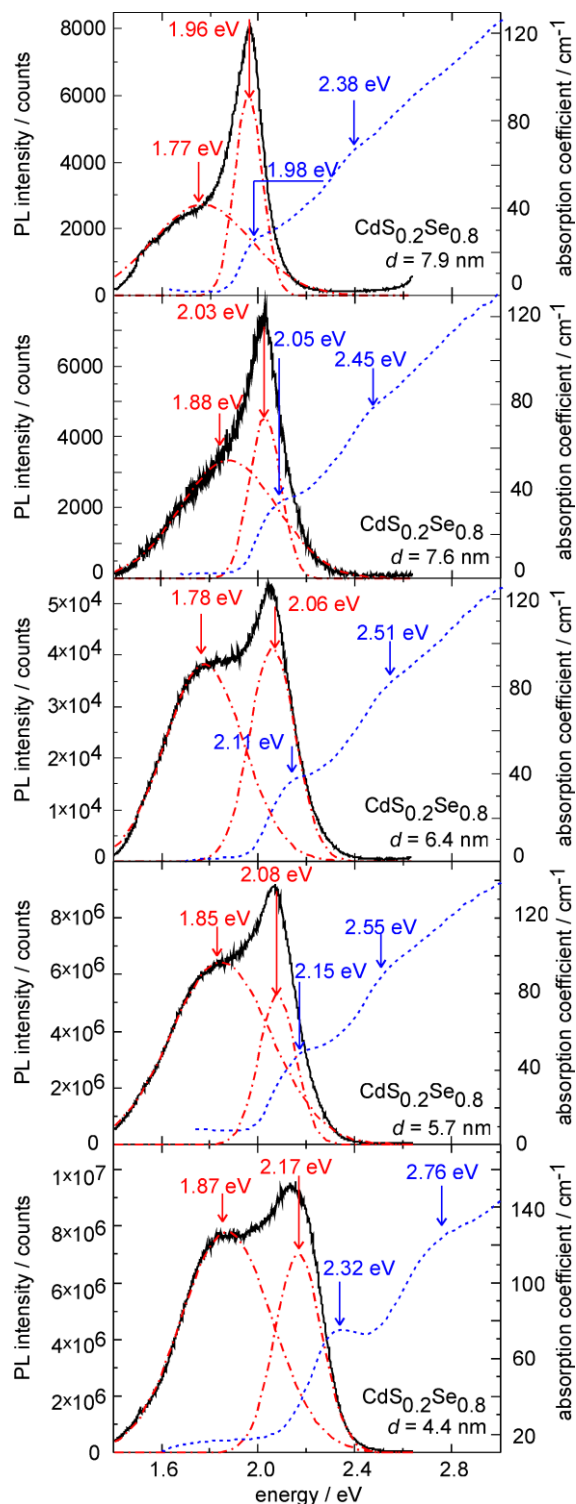

Fig. 1 – Optical absorption (short-dashed lines) and PL (solid lines) spectra of $CdS_{0.2}Se_{0.8}$ nanocrystals of various size embedded in borosilicate glass measured at room temperature. Dash-dotted lines show fits of the PL spectra by two Gaussian components with the corresponding peak spectral positions being indicated

state fine structure due to the structural anisotropy and electron-hole exchange interaction [28]. An alternative explanation, especially regarding the PL band width, is based on exciton-acoustic phonon scattering [29].

A considerably broader band, significantly shifted towards lower energies, is usually attributed to recombination mediated by surface states [5, 7, 12], in particular chalcogen (S^- or Se^-) traps or V^{2+} anion vacancies [30, 31].

The dependence of the PL peak energy positions as well as of the first absorption peak energy on the $CdS_{0.2}Se_{0.8}$ nanocrystal average size is shown in Fig. 2. It can clearly be seen that with increasing $CdS_{0.2}Se_{0.8}$ nanocrystal size, the higher-energy PL peak shifts downward in energy, following the HOMO-LUMO energy gap. However, the Stokes shift (the energy difference between the first absorption maximum and the near-bandgap emission peak) decreases with increasing nanocrystal size from 0.15 eV (for $d = 4.4$ nm) to 0.02 eV (for $d = 7.9$ nm). This is typical for II-VI nanocrystals [32-34] and both the "dark exciton" and exciton–acoustic phonon coupling models were invoked for the explanation [33].
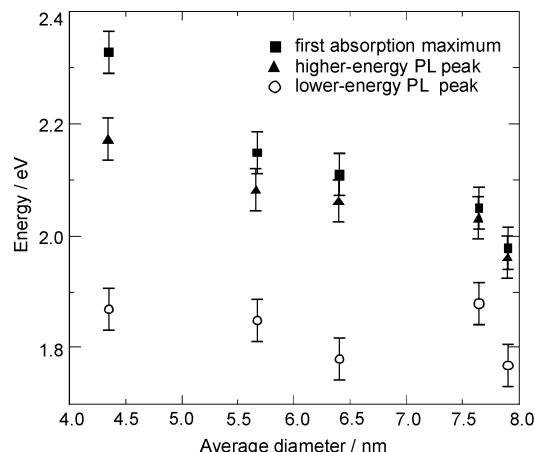

Fig. 2 – Dependence of the spectral positions of the PL maxima and the first absorption peak in $CdS_{0.2}Se_{0.8}$ nanocrystals on the nanocrystal size

Meanwhile, the lower-energy PL peak position does not exhibit any distinct trend with size increase. The interval of its variation (1.77-1.85 eV) is relatively narrow in comparison with its width (near 0.4 eV) which is much larger than for the higher-energy PL band. Its independence on the nanoparticle size is consistent with the origin of this band being related to chalcogen vacancies [35]. The idea of vacancies involved in the radiative recombination and mostly localized at the nanocrystal surface (interface with the matrix) is supported by the observed redistribution of the PL band intensities in favour of the lower-energy band (Fig. 1) with decreasing size, *i.e.* when the nanocrystal surface-to-volume ratio increases. It should be noted that the PL properties do not depend on the nanoparticle size also in the case when they contain deep impurities with strongly localized electrons and holes [36]. Though in our case no intentional doping of the samples was performed, appearance of deep-level impurities could not be totally prevented due to the diffusion-limited growth technique being used.
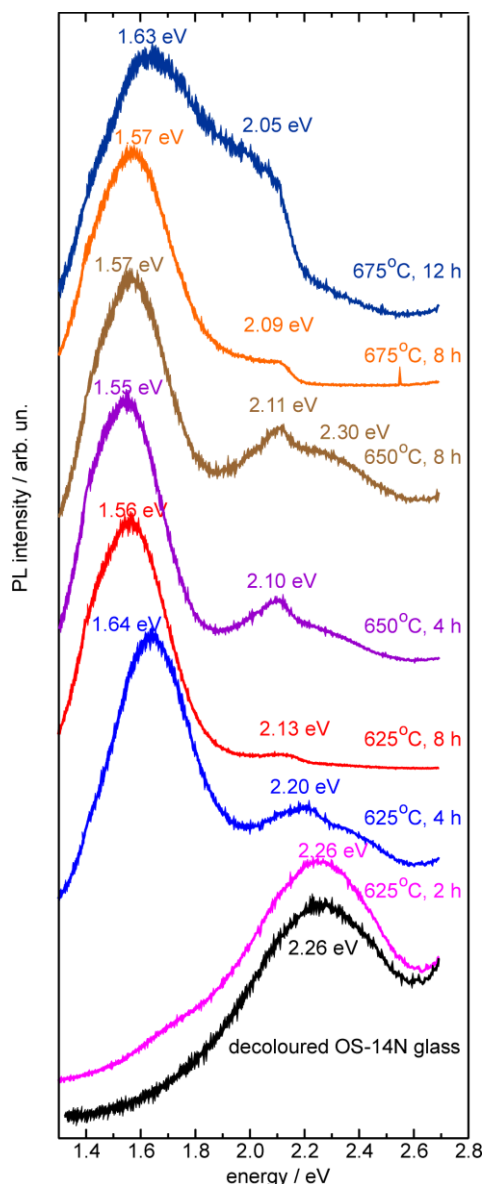
Fig. 3 – PL spectra of decoloured OS-14N glass and samples with $CdS_{0.52}Se_{0.48}$ nanocrystals of various size obtained by annealing at 625 to 675 °C. The annealing temperature and duration are shown in the figure for each sample

Figure 3 shows the PL spectra of the samples prepared from the OS-14N glass by thermal treatment. The decoloured glass without semiconductor nanocrystals reveals a PL maximum at 2.26 eV. At the least intense annealing (625 °C, 2 h) the PL spectrum remains almost unchanged, with a very weak shoulder near 1.6 eV. Meanwhile, Raman measurements performed for the sample annealed for 2 h at 625 °C reveal CdSe-like and CdS-like LO phonon peaks near 201 and 290 cm^{-1}, respectively (though less pronounced than for more intensely annealed samples). This is the evidence for the presence of $CdS_{0.52}Se_{0.48}$ nanocrystals already in the least intensely annealed sample, and the very weak shoulder near 1.6 eV can be related to the nanocrystal PL. With increasing annealing duration and temperature, the average nanocrystal size increases (at the early stage the amount of the nanocrystals increases as well) [24], and the features in the PL spec-

tra corresponding to $CdS_{0.52}Se_{0.48}$ nanocrystals not only become more pronounced, but also vary depending on the average nanocrystal size (Fig. 3). Though for some samples a weak glass matrix PL shoulder near 2.30 eV is still revealed, the spectra are clearly dominated by the nanocrystal-related bands, the size behaviour of which is similar to that observed from Fig. 1. Namely, the less intense higher-energy PL band clearly shifts towards lower energies with increasing $CdS_{0.52}Se_{0.48}$ nanocrystal size while the position of the intense lower-energy PL maximum fluctuates in the range 1.55-1.64 eV independently of the nanocrystal size.

As shown in Fig. 4, the position of the surface-mediated PL band remains within the same energy range for different $CdS_{1-x}Se_x$ nanocrystal compositions. Meanwhile, the higher-energy PL maximum clearly shifts down with x, following the optical absorption peak position. It is seen that for small nanocrystals with lower selenium concentration the surface-mediated peak totally dominates in the PL spectrum.
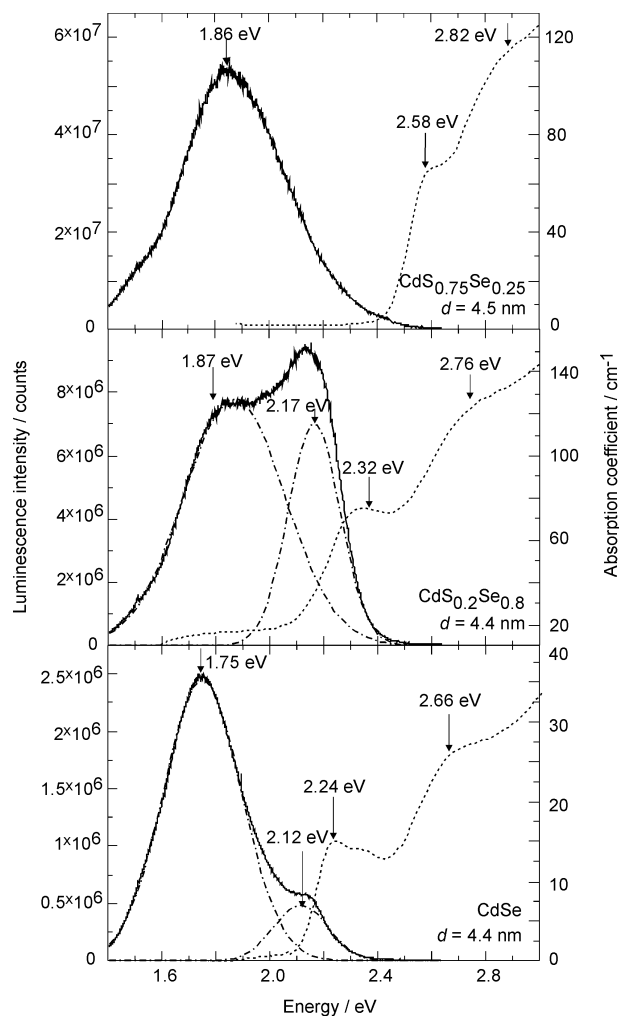

Fig. 4 – Optical absorption (short-dashed lines) and PL (solid lines) spectra of $CdS_{1-x}Se_x$ nanocrystals of similar size and different composition embedded in borosilicate glass measured at room temperature. Dash-and-dotted lines show fits of the PL spectra by two Gaussian components, the corresponding peak spectral positions being indicated

The TSL spectra of the borosilicate glass-embedded $CdS_{1-x}Se_x$ nanocrystals of a similar size ($d = 4.4$–4.5 nm) with different chemical composition, shown in Fig. 5, reveal a basically similar compositional behaviour of the luminescence spectrum, as shown above for the PL spectra. Note that for the TSL measurements signal-to-noise ratio is much lower than for the PL data. Similarly, the observed TSL spectra appear to be
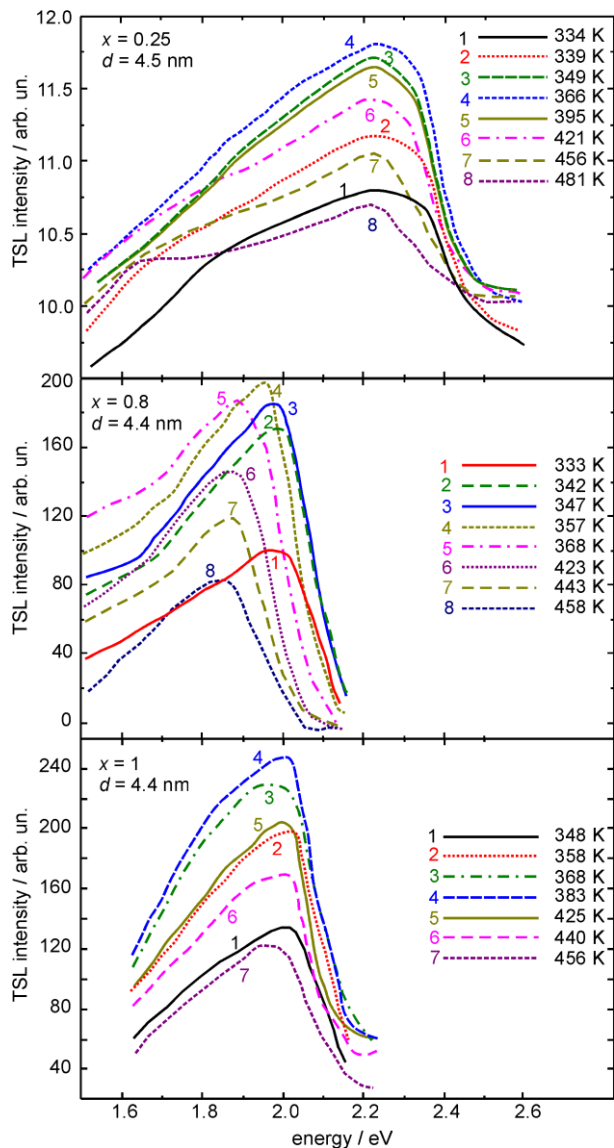

Fig. 5 – Spectral dependences of TSL of borosilicate glass-embedded $CdS_{1-x}Se_x$ nanocrystals of similar size and different composition, irradiated with an X-ray dose of $D = 1000$ Gy

composed of at least two maxima (Fig. 6) which seem broader than the PL bands. For the sample with $CdS_{0.75}Se_{0.25}$ nanocrystals ($d = 4.5$ nm) the observed initial TSL spectrum (Fig. 6) consists of three peaks, the highest-energy of them (2.31 eV) is evidently related to the glass matrix luminescence (cf. the PL band at 2.26 eV observed for the decoloured glass in Fig. 3). Besides, as can be seen from the comparison of the deconvoluted PL and TSL bands for the same samples, shown in Figs. 4 and 6, respectively, the constituent peak positions for the PL an TSL differ from each oth-

er. For some samples (e.g. $x = 0.25$, $d = 4.5$ nm) the TSL spectrum is richer, revealing more features than the PL one. This indicates that PL and TSL spectra of the glass-embedded $CdS_{1-x}Se_x$ nanocrystals result from recombination processes with the participation of different energy levels. In particular, the TSL processes can be affected by X-ray irradiation-induced ionization of $CdS_{1-x}Se_x$ nanocrystals which capture electrons from the irradiation-excited electron-hole pairs, while holes are being trapped by radiation-induced hole traps in the glass matrix. Since the captured electrons occupy the lowest energy states and disable the corresponding optical transitions [37], this effect can lead as well to the changes in the radiative transition energies.
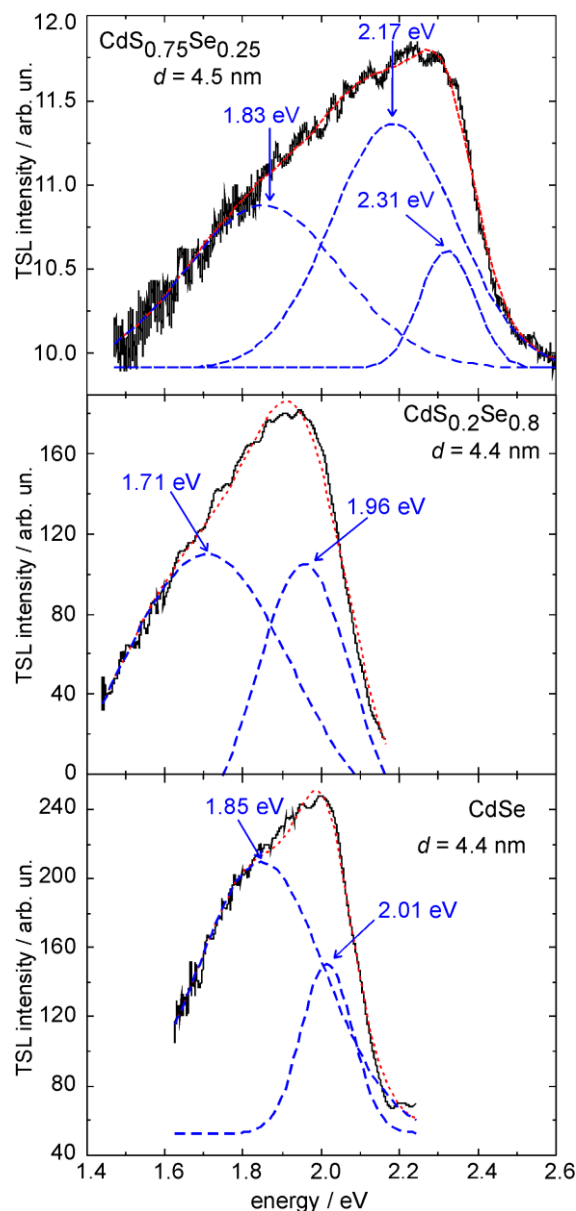

Fig. 6 – Typical experimental TSL spectra of borosilicate glass-embedded $CdS_{1-x}Se_x$ nanocrystals of similar size and different composition (solid lines) and their approximation by two or three Gaussian contours (dashed lines). The dotted lines show the total contribution of the two Gaussian contours
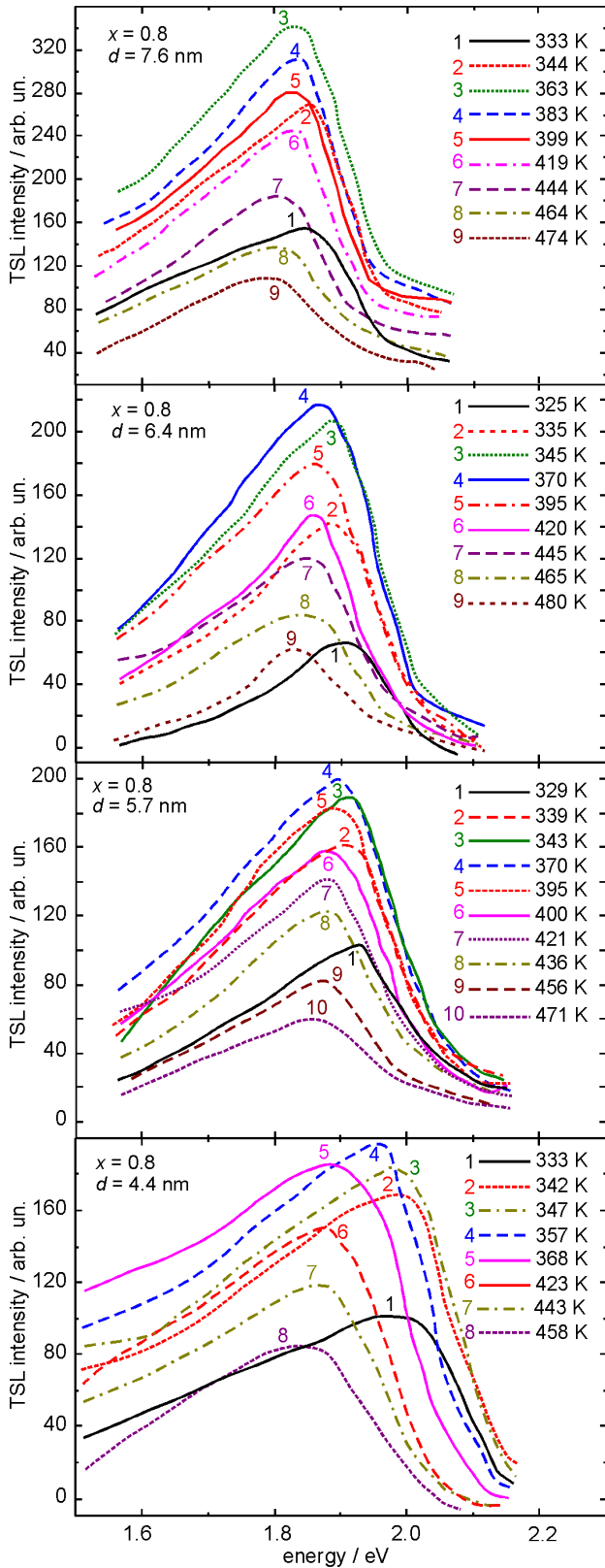
Fig. 7 – TSL spectra of CdS$_{0.2}$Se$_{0.8}$ nanocrystals of various size, irradiated with an X-ray dose of $D = 1000$ Gy.

Similarly to the PL, the TSL spectra of the glass-embedded CdS$_{1-x}$Se$_x$ nanocrystals shift towards higher energies with the size decrease which is illustrated by Fig. 7. However, this trend is not as distinct as for the PL spectra, which can be related to several factors,

especially to the temperature variation of the TSL peak spectral positions and the compositional and size dependence of the TSL temperature maximum which will be discussed below.

It is clearly seen from Figs. 5 and 7 that the TSL intensity exhibits an increase with temperature up to 360-370 K, followed by a subsequent decrease with further heating. The corresponding dependences of the overall TSL intensity within the measured range on the measurement temperature are shown in Fig. 8. Since the observed TSL band spectral positions exhibit clear dependence on the nanocrystal composition and size (Figs. 5 and 7, respectively), they can be related to the processes of radiative recombination in CdS$_{1-x}$Se$_x$ nanocrystals. Note that the most intense luminescence peaks in borosilicate glasses are known to be observed mainly at higher energies (above 2.6 eV) [38], hence their effect on the TSL spectra of the nanocrystals should be negligible.
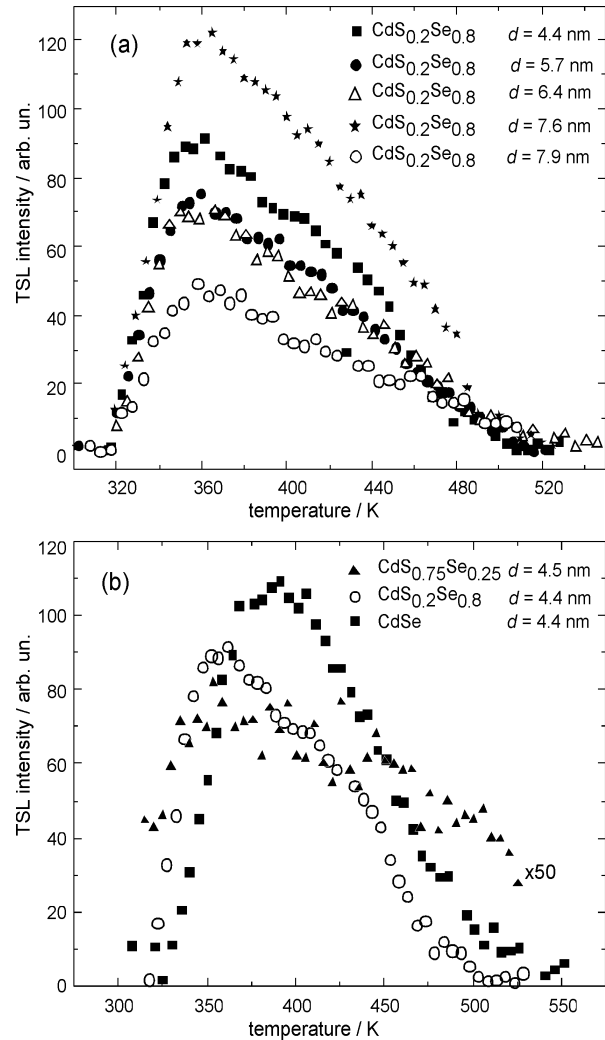

Fig. 8 – Temperature dependences of the total TSL intensity for the borosilicate glass-embedded CdS$_{0.2}$Se$_{0.8}$ nanocrystals of different size (a) and CdS$_{1-x}$Se$_x$ nanocrystals of similar size and different composition (b), irradiated with an X-ray dose of $D = 1000$ Gy

It is worth mentioning that we could not observe any clear dependence of the TSL peak temperature on

the $CdS_{1-x}Se_x$ nanocrystal size and composition. The only sample with CdSe nanocrystals with $d = 4.4$ nm exhibits the maximum TSL temperature near 380 K while all other samples under study show the maximal TSL near 360-370 K. Note that our data do not match those of Dekanozishvili *et al.* who observe a TSL peak near 420 K for glass-embedded CdSe nanocrystals [22] as well those of Miyoshi *et al.* where a much higher value (470 K) is reported for glass-embedded CdS nanocrystals [20]. At present, we cannot find an unambiguous explanation for this discrepancy which can be related, in particular, to the differences in the nanocrystal size and composition as well as in the glass matrix. However, the reason for the discrepancies in the maximum TSL temperatures between our data and those of Refs. 20 and 22 can also be related to the complicated character of the TSL band.
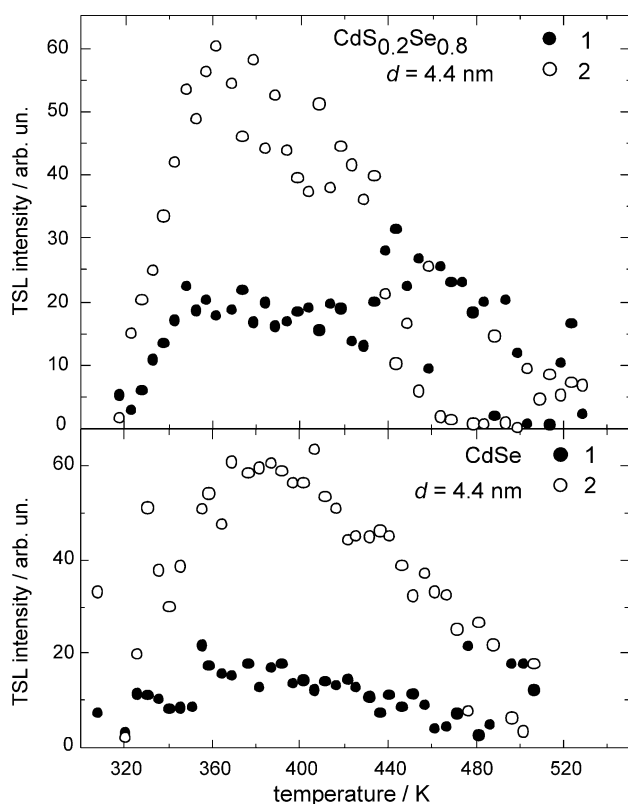

Fig. 9 – Temperature dependences of the lower-energy (dark symbols) and higher-energy (open symbols) TSL band intensities for the borosilicate glass-embedded $CdS_{1-x}Se_x$ nanocrystals of similar size and different composition, irradiated with an X-ray dose of $D = 1000$ Gy

A careful look at the spectra in Fig. 7 makes one notice that the overall TSL intensity increase (up to 360-380 K) and subsequent decrease (with further heating) is accompanied by a slight downward shift of the TSL maximum energy position. Evidently, such behaviour can be related to a different temperature dependence of the higher-energy and lower-energy luminescence bands, illustrated by Fig. 9. As seen from the figure, the intensity of the lower-energy TSL band is almost the same in a quite broad temperature range (roughly 350 to 450 K, somewhat varying for the samples with different nanocrystal composition). Meanwhile, the intensity of the higher-energy band exhibits a clearly defined maximum at 360-380 K. One may conclude that it is the higher-energy band which determines the temperature behaviour of the glass-embedded $CdS_{1-x}Se_x$ nanocrystal TSL. A more detailed TSL study with better spectral resolution and signal-to-noise ratio as well as a broader set of samples with $CdS_{1-x}Se_x$ nanocrystals and a broader irradiation dose range is required to judge upon the nature and transformation of recombination centres responsible for the two TSL bands and thereby to provide recommendations on the possible application of these materials for radiation measurements.

4. CONCLUSIONS

PL and TSL spectra of $CdS_{1-x}Se_x$ nanocrystals of different size and composition embedded in borosilicate glass were studied. The near-edge PL band energy is observed to decrease with the nanocrystal size and selenium content, as well as the Stokes shift between the PL maximum and the first absorption peak position. The lower-energy PL peak position, practically independent of the $CdS_{1-x}Se_x$ nanocrystal size and composition as well as the increase of the relative intensity of this peak with decreasing nanocrystal size confirm it to be related with radiative recombination processes involving defect states localized on the nanocrystal surface. The TSL spectral dependences reveal different temperature behaviour for the higher-energy band exhibiting a rather sharp maximum at 360-380 K, dependent of the nanocrystal size and composition) and the lower-energy peak, the intensity of which varies only slightly in a broad temperature range, roughly from 350 to 450 K.

Спектри фото- і термостимульованої люмінесценції нанокристалів CdS$_{1-x}$Se$_x$, вкраплених у боросилікатне скло

Ю.М. Ажнюк[1], В.В. Лопушанський[1], М.В. Примак[1], К.П. Попович[1], А.М. Соломон[1], О.В. Гомоннай[1], Д.Р.Т. Цан[2]

[1] *Інститут електронної фізики НАН України, вул. Університетська, 21, 88017 Ужгород, Україна*

[2] *Кемніцький технічний університет, D-09107 Кемніц, Німеччина*

Досліджено фотолюмінесценцію (ФЛ) і термостимульовану люмінесценцію (ТСЛ) нанокристалів CdS$_{1-x}$Se$_x$, вкраплених у боросилікатне скло. Отримано залежності спектрального положення смуг прикрайової та пов'язаної з поверхневими рівнями ФЛ від хімічного складу та розміру нанокристалів. Обговорюється різна температурна поведінка більш високоенергетичної смуги ТСЛ (максимум при 360-380 K, залежно від складу і розміру нанокристалів) і низькоенергетичної смуги (широкий максимум в інтервалі 350-450 K).

Ключові слова: Напівпровідникові нанокристали, Оптичне поглинання, Фотолюмінесценція, Термостимульована люмінесценція.

Спектры фото- и термостимулированной люминесценции нанокристаллов CdS$_{1-x}$Se$_x$, диспергированных в боросиликатном стекле

Ю.М. Ажнюк[1], В.В. Лопушанский[1], М.В. Примак[1], К.П. Попович[1], А.М. Соломон[1], А.В. Гомоннай[1], Д.Р.Т. Цан[2]

[1] *Институт электронной физики НАН Украины, ул. Университетська, 21, 88017 Ужгород, Украина*

[2] *Кемницкий технический университет, D-09107 Кемниц, Германия*

Исследована фотолюминесценция (ФЛ) и термостимулированная люминесценция (ТСЛ) нанокристаллов CdS$_{1-x}$Se$_x$, диспергированных в боросиликатном стекле. Получены зависимости спектрального положения полос прикраевой и связанной с поверхностными уровнями ФЛ от химического состава и размера нанокристаллов. Обсуждается разное температурное поведение более высокоэнергетической полосы ТСЛ (максимум при 360-380 K в звисимости от состава и размера нанокристаллов) и низкоэнергетической полосы (широкий максимум в интервале 350-450 K).

Ключевые слова: Полупроводниковые нанокристаллы, Оптическое поглощение, Фотолюминесценция, Термостимулированная люминесценция.

REFERENCES

1. H. S. Nalwa (Ed.), *Nanostructured Materials and Nanotechnology* (Academic Press, San Diego, 2002).
2. C. Klingshirn, *Landolt-Börnstein – Group III Condensed Matter, Optical Properties. Part 2 Volume 34C2* (Springer , Berlin – Hedelberg – New York, 2004).
3. A. Fu, W. Gu, C. Larabell, A. P. Alivisatos, *Current Opinion Neurobiology* **15**, 568 (2005).
4. R. C. Somers, M. G. Bawendi, D. G. Nocera, *Chem. Soc. Rev.* **36**, 579 (2007).
5. N.F. Borrelli, D. Hall, H. Holland, D. Smith, *J. Appl. Phys.* **61**, 5399 (1987).
6. A. Ekimov, *J. Luminesc.* **70**, 1 (1996).
7. J. Warnock, D.D. Awschalom, *Phys. Rev. B* **32**, 5529 (1985).
8. G. Mei, *J. Phys: Condens. Matt.* **4**, 7521 (1992).
9. M. Ya. Valakh, N.R. Kulish, V.P. Kunets, M.P. Lisitsa, G.Yu. Rudko, *Ukr. J. Phys.* **38**, 1667 (1993).
10. M. Ivanda, T. Bischof, G. Lermann, A. Materny, W. Kiefer, *J. Appl. Phys.* **82**, 3116 (1997).
11. Q. Shen, K. Abe, T. Shigenari, T. Toyoda, *J. Luminesc.* **87–89**, 444 (2000).
12. P. Verma, G. Irmer, J. Monecke, *J. Phys.: Condens. Matter* **12**, 1097 (2000).
13. Yu.M. Azhniuk, A.G. Milekhin, A.V. Gomonnai, V.V. Lopushansky, V.O. Yukhymchuk, S. Schulze, E.I. Zenkevich, D.R.T. Zahn, *J. Phys.: Condens. Matter* **16**, 9069 (2004).
14. S. Santhi, E. Bernstein, F. Paille, *J. Luminesc.* 117, 101 (2006).
15. V.V. Ushakov, A.S. Aronin, V.A. Karavanskii, A.A. Gippius, *Fiz. Tverd. Tela* **51**, 2036 (2009) [English translation: *Phys. Solid State* **51**, 2161 (2009)].
16. B. Can Ömür, A. Aşıkoğlu, Ç. Allahverdi, M. H. Yükselici, *J. Mater. Sci.* **45**, 112 (2010).
17. P. Němec, F. Trojánek, P. Malý, *Phys. Rev. B* **52**, R8605 (1995).
18. P. Němec, P. Malý, *J. Appl. Phys.* **87**, 3342 (2000).
19. D. Matsuura, Y. Kanemitsu, T. Kushida, C. W. White, J.D. Budai, A. Meldrum, *Jpn. J. Appl. Phys.* **40**, 2092 (2001).
20. T. Miyoshi, H. Sera, N. Matsuo, T. Kaneda, *Jpn. J. Appl. Phys.* **40**, 2327 (2001).
21. T. Miyoshi, Y. Makidera, T. Kawamura, S. Kashima, N. Matsuo, T. Kaneda, *Jpn. J. Appl. Phys.* **41**, 5262 (2002).
22. G. Dekanozishvili, D. Driaev, K. Kalabegishvili, V. Kvatchadze, *J. Luminesc.* **129**, 1154 (2009).
23. Yu.M. Azhniuk, V.V. Lopushansky, A.V. Gomonnai, V.O. Yukhymchuk, I.I. Turok, Ya.I. Studenyak, *J. Phys. Chem. Sol.* **69**, 139 (2008).

24. Yu. M. Azhniuk, A. V. Gomonnai, Yu. I. Hutych, V. V. Lopushansky, I. I. Turok, V. O. Yukhymchuk, D. R. T. Zahn, *J. Crystal Growth* **312**, 1709 (2010).
25. V.I. Lyamayev, *Meas. Sci. Technol.* **17** (issue 12), 75 (2006).
26. A.I. Ekimov, E. Hache, M.C. Schanne-Klein, D. Ricard, C. Flytzanis, I.A. Kudryavtsev, T.V. Yazeva, A.V. Rodina, Al.L. Efros, *J. Opt. Soc. Amer. B* **10**, 100 (1993).
27. H. H. von Grünberg, *Phys. Rev. B* **55**, 2293 (1997).
28. M. Nirmal, D.J. Norris, M. Kuno, M.G. Bawendi, Al.L. Efros, M. Rosen, *Phys. Rev. Lett.* **75**, 3728 (1995).
29. D. Valerini, A. Creti, M. Lomascolo, L. Manna, R. Cingolani, M. Anni, *Phys. Rev.B* **71**, 235409 (2005).
30. B. Liu, G. Q. Xu, L. M. Gan, C.H. Chew, W. S. Li, Z. X. Shen, *J. Appl. Phys.* **89**, 1059 (2001).
31. P.K. Khanna, R.R. Gokhale, V.V.V.S. Subbarao, N. Singh, K.-W. Jun, B.K. Das, *Mater. Chem. Phys.* **94**, 454 (2005).
32. Z. Yu, J. Li, D.B. O'Connor, L.-W. Wang, P.F. Barbara, *J. Phys. Chem. B* **107**, 5670 (2003).
33. T.J. Liptay, L.F. Marshall, P.S. Rao, R.J. Ram, M.G. Bawendi, *Phys. Rev. B* **76**, 155314 (2007).
34. A.E. Raevskaya, A.L. Stroyuk, S.Ya. Kuchmiy, V.M. Dzhagan, M.Ya. Valakh, D.R.T. Zahn, *J. Phys.: Condens. Matter* **19**, 386237 (2007).
35. A.L. Stroyuk, V.M. Dzhagan, D.R.T. Zahn, C. von Borczyskowski, *Theor. and Experim. Chem.* **43**, 297 (2007).
36. Y. Kanemitsu, A. Ishizumi, *J. Luminesc.* **119–120**, 161 (2006).
37. Yu.M. Azhniuk, M.V. Prymak, V.V. Lopushansky, A.M. Solomon, Yu.I. Hutych, A.V. Gomonnai, D.R.T. Zahn, *J. Appl. Phys.* **107**, 113528 (2010).
38. A.V. Gomonnai, A.M. Solomon, Yu.M. Azhniuk, M. Kranjčec, V.V. Lopushansky, I.G. Megela, *J. Optoelectron. Adv. Mater.* **3**, 509 (2001).